Spatially heterogeneous dynamics and dynamic facilitation in a model of viscous silica

Michael Vogel* and Sharon C. Glotzer
Departments of Chemical Engineering and Materials Science and Engineering, University of Michigan, 2300 Hayward, Ann Arbor, MI, 48109, USA
(Dated: February 2, 2008)

Performing molecular dynamics simulations, we find that the structural relaxation dynamics of viscous silica, the prototype of a strong glass former, are spatially heterogeneous and cannot be understood as a statistical bond breaking process. Further, we show that high particle mobility predominantly propagates continuously through the melt, supporting the concept of dynamic facilitation emphasized in recent theoretical work.

PACS numbers: 66.30.Dn

One of the most challenging problems of condensed matter physics is still the understanding of the tremendous slowing down of molecular dynamics in supercooled liquids approaching the glass transition temperature T_g, which is not accompanied by a substantial change of the structure. In the past, several theories have been invoked to rationalize this behavior. The mode coupling theory [1] describes many experimental findings at high temperatures, but it predicts a power-law divergence of relaxation times at a critical temperature T_{MCT} significantly above T_g. The Adam-Gibbs approach [2] sees the glass transition phenomenon as resulting from an increase of cooperativity of molecular dynamics when the temperature is decreased. However, the underlying microscopic picture is not well established.

Very recently, Garrahan and Chandler (GC) [3, 4] introduced a microscopic model of supercooled liquids, which is based on three central ideas: (i) Particle mobility is sparse and dynamics are spatially heterogeneous at times intermediate between ballistic and diffusive motion. (ii) Particle mobility is the result of dynamic facilitation, i.e., mobile particles assist their neighbors to become mobile. (iii) Mobility propagation carries a direction, the persistence length of which is larger for fragile than for strong glass formers [5]. For non-strong liquids, the existence of spatially heterogeneous dynamics (SHD) is well established by experiment [6, 7, 8] and simulation [9, 10, 11, 12, 13, 14, 15, 16, 17]. Further, it was observed [11, 13, 15, 17] that groups of particles follow one another along string-like paths. GC proposed [4] that dynamic facilitation and persistence of particle-flow direction manifest themselves in this string-like motion. For strong liquids, like silica, experimental studies are rare due to the high T_g of these network-forming materials. However, it is usually argued that the structural relaxation can be understood as simple activated bond breaking process.

Here, we perform molecular dynamics (MD) simulations to study the relaxation dynamics of viscous silica, the prototype of a strong glass former [5]. In particular, we critically test the ideas of the GC model. For our simulations, we apply the BKS potential [18], which is commonly used to reproduce structural and dynamical properties of viscous silica [19, 20, 21, 22, 23, 24]. We show that the relaxation dynamics in BKS silica are spatially heterogeneous, indicating a complex nature of this dynamical process. Further, we demonstrate quantitatively that dynamic facilitation is not only relevant in spin models [25], but also in a viscous equilibrium liquid. Finally, we show that string-like motion is less important in BKS silica than in non-strong liquids, suggesting a reduced persistence of particle-flow direction, in agreement with the GC model. To arrive at these results, we follow Horbach and Kob [22, 23] and perform simulations in the NVE ensemble with $\rho = 2.37\,\mathrm{g/cm^3}$ and $N = 8016$, which is sufficiently large so as to avoid finite size effects at the studied temperatures. Further simulation details can be found in Refs. [22, 23, 26].

Consistent with experimental results [27], the temperature dependence of the transport coefficients in BKS silica changes from a non-Arrhenius behavior at high T to an Arrhenius behavior at low T, where the crossover occurs in the vicinity of T_{MCT} [22, 23, 24]. This result is confirmed by our analysis, see Fig. 1(a). Using the literature value $T_{MCT} = 3330\,\mathrm{K}$ [22, 23], we find that the diffusion coefficients D for both oxygen and silicon vary according to a power-law [1], $D \propto (T - T_{MCT})^{\gamma}$, at high T, whereas Arrhenius laws are observed at $T \lesssim T_{MCT}$. The activation energies $E_a = 4.7\mathrm{eV}$ and $E_a = 5.0\mathrm{eV}$ for the oxygen and silicon atoms, respectively, are consistent with previous results from simulations [22, 23] and experiments [28, 29]. Following the time evolution of the mean square displacement, $r^2(\Delta t)$, in Fig. 1(b), three distinct time regimes can be distinguished at sufficiently low T [22]. Ballistic and diffusive motion at short and long times, respectively, are separated by a pronounced caging regime [1], where the particles are temporarily trapped in cages formed by their neighbors.

To demonstrate that dynamics in silica are spatially heterogenous, we show that highly mobile particles form clusters larger than predicted from random statistics. Following previous work [13, 14, 15, 16], we characterize the particle mobility in a time interval Δt by the scalar displacement and select the 5% most mobile particles for

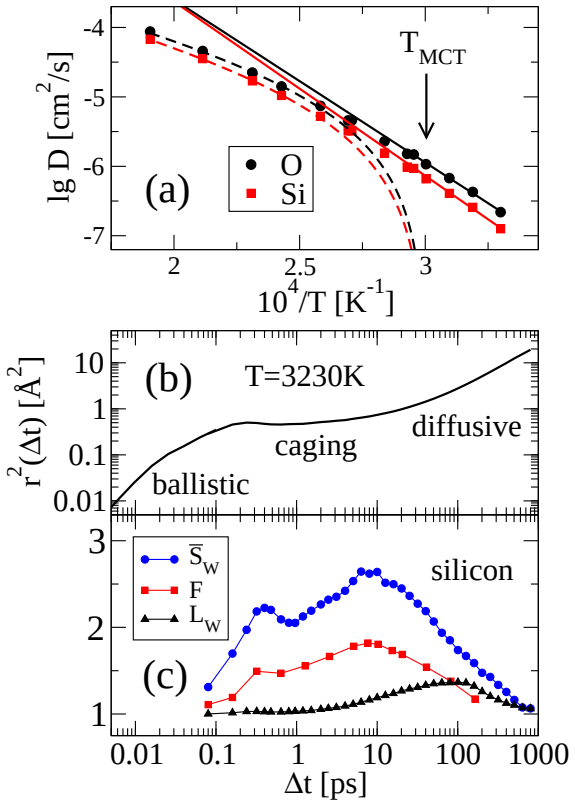

FIG. 1: (a) Diffusion coefficients $D(1/T)$ for the oxygen and silicon atoms. Dashed lines: Power-laws $D \propto (T-3330\,\mathrm{K})^{\gamma}$ with $\gamma = 2.0$ and $\gamma = 2.1$ for the oxygen and silicon atoms, respectively. Solid lines: Arrhenius laws with activation energies $E_a = 4.7\,\mathrm{eV}$ for oxygen and $E_a = 5.0\,\mathrm{eV}$ for silicon. (b) Mean square displacement, $r^2(\Delta t)$, for the silicon atoms at $T = 3230\,\mathrm{K}$. (c) Normalized mean cluster size $\overline{S}_W(\Delta t)$, mean string length $L_W(\Delta t)$ and the dynamic facilitation effect $F(\Delta t)$, cf. Eq. 2, for the silicon atoms at $T = 3230\,\mathrm{K}$.

further analysis. Then, we define a cluster as a group of the most mobile particles that reside in the first neighbor shell of each other. From the probability distribution $P_S(n;\Delta t)$ of finding a cluster of size n within a time interval Δt we calculate the weight-averaged mean cluster size

$$S_W(\Delta t) = \frac{\sum_n n^2\, P_S(n;\Delta t)}{\sum_n n\, P_S(n;\Delta t)}. \qquad (1)$$

This quantity measures the average size of a cluster to which a mobile particle belongs. To eliminate the random contribution, we discuss the normalized size $\overline{S}_W(\Delta t) = S_W(\Delta t)/S_W^*$, where S_W^* is the value that results when 5% of the particles are selected irrespective of their mobility. Our conclusions are unchanged, when the fraction of mobile particles is varied over a meaningful range [26].

Figure 1(c) shows $\overline{S}_W(\Delta t)$ for the silicon atoms at $T = 3230\,\mathrm{K}$. We see that the mean cluster size exhibits two maxima, indicating the existence of two spatially heterogeneous dynamical processes. The secondary and primary maxima are located at the crossovers from the ballistic to the caging regime and from the caging to the diffusive regime, respectively. In Fig. 2, we depict the temperature dependence of $\overline{S}_W(\Delta t)$ for the oxygen atoms. The behavior of the primary maximum is analogous to that for simple liquids and polymer melts [14, 15]. Both the peak time t_S and the peak height $\overline{S}_W(t_S)$ increase upon cooling. Here, the growth of the clusters continues in the temperature range where D follows an Arrhenius law, cf. Fig. 1(a). For $T \approx T_{MCT}$, the mean cluster sizes $\overline{S}_W(t_S)$ for the oxygen and silicon are located at the lower end of the spectrum of values reported for non-strong liquids [13, 14, 15, 16]. Hence, at times when the particles escape from their cages, BKS silica exhibits SHD, which is at least qualitatively comparable to that of non-strong liquids. The position of the secondary maximum is temperature independent so that both peaks merge for $T \gtrsim 4000\,\mathrm{K}$. In studies of water [16], an analogous secondary peak was observed and ascribed to "strong correlations in the vibrational motion of first-neighbor molecules". For BKS silica, a Boson peak was found at the crossover from the ballistic to the caging regime [21]. Therefore, we speculate that this phenomenon leads to the secondary peak and, hence, can be characterized as localized, cooperative vibrational motion.

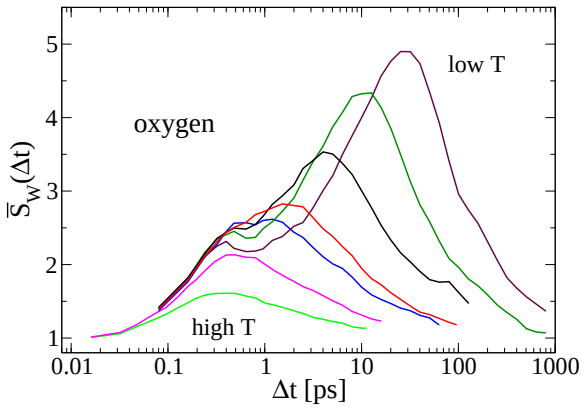

FIG. 2: Normalized mean cluster size, $\overline{S}_W(\Delta t)$, for the oxygen atoms at various temperatures (5250 K, 4330 K, 3870 K, 3690 K, 3390 K, 3230 K, 3030 K).

String-like motion was found to be an important channel of relaxation in fragile liquids [11, 13, 15, 17]. To study this type of motion for silica, we follow Donati *et al.* [11] and construct strings by connecting any two particles i and j of the same atomic species if

$$\min[\,|\vec{r}_i(t_0) - \vec{r}_j(t_0+\Delta t)|, |\vec{r}_i(t_0+\Delta t) - \vec{r}_j(t_0)|\,] < \delta.$$

is valid for the particle positions at two different times. To ensure that one particle has moved and another particle has occupied its position, δ is set to about 55% of the respective interparticle distance. In Fig. 1(c), we include the weight-averaged mean string length $L_W(\Delta t)$,

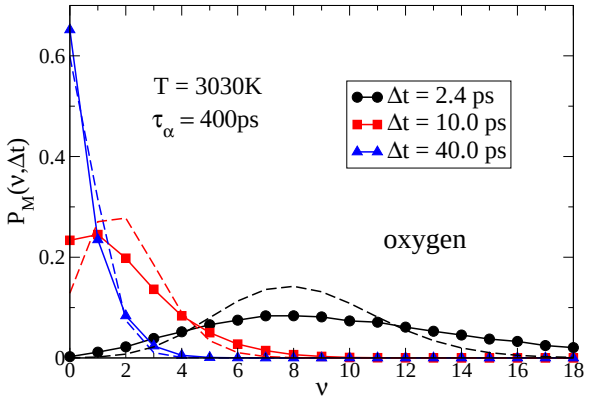

FIG. 3: Probability distributions $P_M(\nu, \Delta t)$ of finding an oxygen atom ν times mobile when dividing τ_α into time intervals Δt and identifying the mobile particles in each interval. The dashed lines are the corresponding expectations, $P^*_M(\nu, \Delta t)$, for a random selection of mobile particles in each interval. At the studied temperature $T = 3030\,\mathrm{K}$, we find $t_S \approx 10\,\mathrm{ps}$.

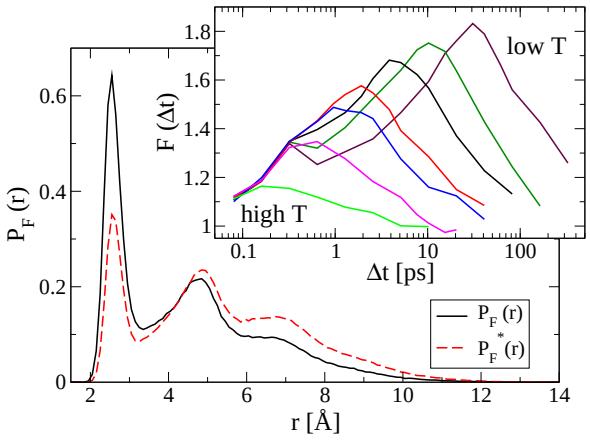

FIG. 4: Probability distribution $P_F(r, \Delta t)$ of finding a smallest distance r between an oxygen atom, which becomes mobile in $\Delta t_{23} = \Delta t$, and any oxygen atom, which was mobile in $\Delta t_{12} = \Delta t$ ($T = 3030\,\mathrm{K}$). $P^*_F(r, \Delta t)$ results when the mobile particles in Δt_{23} are randomly selected from the non-mobile particles in Δt_{12}. The distance is calculated based on the configuration at the time t_2, separating both time intervals. The inset shows the temperature dependence of $F(\Delta t)$ quantifying the strength of dynamic facilitation for the oxygen atoms, cf. Eq. 2. The temperatures are 5250 K, 4330 K, 3870 K, 3690 K, 3390 K, 3230 K and 3030 K.

calculated for the silicon atoms at $T = 3230\,\mathrm{K}$ in analogy with Eq. 1. From the small values $L_W(\Delta t) \approx 1$, it is clear that string-like motion is of little relevance for the relaxation of the silicon atoms. Though the strings are somewhat longer for the oxygen atoms, e.g. a maximum value $L_W(t_L) = 1.5$ is found at $T = 3230\,\mathrm{K}$, they are still much smaller than in non-strong liquids, where $L_W(t_L) > 3$ for $T \approx T_{MCT}$ [15, 17]. Thus, we conclude that string-like motion in BKS silica is suppressed due to the presence of covalent bonds at the studied T.

Having established the existence of dynamic heterogeneities, we now measure their lifetime. For this purpose, we identify the most mobile particles in back-to-back time intervals, $\Delta t_{12} = \Delta t$ and $\Delta t_{23} = \Delta t$, and calculate the probability $P(\Delta t)$ of finding a mobile particle in Δt_{12} still mobile in Δt_{23}. For both atomic species at $T = 3030\,\mathrm{K}$, we find a nearly constant value $P(\Delta t) \approx 0.15$ for Δt in the caging regime, followed by a decrease towards the long-time limit $P(\Delta t \to \infty) = 0.05$. These small values indicate that the fluctuations of the dynamical state are rapid. For the dynamic heterogeneities in non-strong liquids, such short lifetimes were observed both in simulation studies near T_{MCT} [9, 13] and in experimental work near, but not too close to T_g [7, 8, 30].

Next, we investigate the number of times a particular particle is mobile on the time scale of the α-relaxation time τ_α. For this analysis, we divide τ_α into several time intervals Δt, identify the most mobile particles in each interval, and determine the probability distribution $P_M(\nu, \Delta t)$ of finding a particle mobile in ν not necessarily consecutive intervals. Figure 3 shows this distribution for the oxygen atoms at $T = 3030\,\mathrm{K}$. For comparison, we include the distribution $P^*_M(\nu, \Delta t)$, resulting for a random selection of 5% of the particles in the intervals Δt. For $\Delta t \geq t_S$, we find $P_M(\nu) \approx P^*_M(\nu)$ and, hence, the subsets of mobile particles in different intervals are statistically independent. Thus, high particle mobility is not limited to certain regions of the sample, but all particles can belong to a cluster of mobile particles on the time scale of τ_α. Some deviations between $P_M(\nu)$ and $P^*_M(\nu)$ for $\Delta t < t_S$ suggest that the relaxation of a particular region of the sample is not complete on this short timescale, consistent with the continuing growth of the clusters.

Finally, we study whether mobility propagates continuously, as proposed in the GC model, or whether it develops at random positions, as suggested by Stillinger and Hodgdon [31] in the model of flickering fluidized domains. To answer this question, we analyze the relative positions of particles that are mobile in back-to-back time intervals $\Delta t_{12} = \Delta t$ and $\Delta t_{23} = \Delta t$, respectively. Specifically, we calculate the probability distribution $P_F(r, \Delta t)$ of finding a smallest distance r between a particle that is mobile in Δt_{23}, but not in Δt_{12}, and any of the mobile particles in Δt_{12}. In Fig. 4, this distribution is shown for the oxygen atoms at $T = 3030\,\mathrm{K}$, where $\Delta t \approx t_S$. For further analysis, we compare these data with the distribution $P^*_F(r, \Delta t)$, which results when the particles used for analysis are randomly selected from the non-mobile oxygen atoms in Δt_{12}. We see that the probability that a neighbor of a mobile oxygen atom becomes mobile in the subsequent time interval is significantly enhanced. Similar results are observed for the silicon atoms and, hence, we can conclude that mobile particles in BKS silica assist their neighbors to become mobile, demonstrating that dynamic facilitation occurs.

The strength of this effect can be quantified based on the quantity

$$F(\Delta t) = \frac{\int_0^{r_{min}} P_F(r,\Delta t)\, dr}{\int_0^{r_{min}} P_F^*(r,\Delta t)\, dr}, \qquad (2)$$

where r_{min} is the first minimum of the pair correlation function. This quantity measures by how much the probability that a neighbor of a mobile particle becomes mobile is enhanced, as compared to the value for a random development of particle mobility. Figure 1(c) displays $F(\Delta t)$ for the silicon atoms at $T = 3230\,\mathrm{K}$. We see that the effect of dynamic facilitation is strongest at a time $t_F \approx t_S$, i.e., when the clusters of mobile particles are largest. Further, $F(t_F) \approx 2$ indicates that dynamic facilitation plays a significant role. The inset of Figure 4 depicts the temperature dependence of $F(\Delta t)$ for the oxygen atoms. It is clearly seen that the relevance of dynamic facilitation strongly increases when T is decreased, suggesting that this effect becomes very important near T_g.

We have shown that the most mobile particles in BKS silica form clusters that are biggest at the crossover from the caging regime to the diffusive regime, indicating that this strong glass former exhibits SHD. Since the most mobile particles show displacements comparable to the interparticle distance at these times [26], we conclude that the structural relaxation of the studied model liquid is not a result of a simple bond breaking process occurring at random positions. Further, we have found that the time and temperature dependence of the mean cluster size are similar to the behavior for simple liquids [13, 14, 15], implying that strong and fragile glass formes exhibit no principal, but at most quantitative differences in the nature of SHD on intermediate timescales. However, cooperative string-like motion is less relevant in BKS silica than in non-network forming liquids [11, 15, 17], suggesting that this dynamical pattern is suppressed by the presence of covalent bonds. Additionally, we have shown that the dynamic heterogeneities in BKS silica are short-lived and spread throughout the sample on the time scale of τ_α. In doing so, the probability that a particle becomes mobile is enhanced in the vicinity of another mobile particle. This tendency for continuous propagation of mobility demonstrates the relevance of dynamic facilitation. The effect of dynamic facilitation is strongest at times when the mean cluster size is maximum and it increases upon cooling, suggesting that this effect is of particular importance when T_g is approached.

In conclusion, we have shown for a strong glass former that (i) dynamics at intermediate timescales are spatially heterogeneous, (ii) dynamic facilitation is important and (iii) the persistence length of particle-flow direction as measured by the relevance of string-like motion is smaller than in fragile liquids. These points are central ideas of the GC model [3, 4] and, hence, our findings support this new approach to the glass transition phenomenon. In addition, our results provide insights into the relaxation dynamics of one of the most important glass formers, which are difficult to obtain from experimental studies.

M. V. acknowledges funding of the DFG through the Emmy Noether-Programm.

* Electronic address: mivogel@umich.edu

[1] W. Götze, L. Sjogren, Rep. Prog. Phys. 55, 241 (1992)
[2] G. Adam and J. H. Gibbs, J. Chem. Phys. 43, 139 (1965)
[3] J. P. Garrahan and D. Chandler, Phys. Rev. Lett. 89, 035704 (2002)
[4] J. P. Garrahan and D. Chandler, Proc. Nat. Acad. Soc. 100, 9710 (2003)
[5] C. A. Angell, In *Relaxations in Complex Systems*, ed. K. L. Ngai, G. B. Wright, p. 3. Naval Research Labaratory
[6] U. Tracht, M. Wilhelm, A. Heuer, H. Feng, K. Schmidt-Rohr and H. W. Spiess, Phys. Rev. Lett. 81, 2727 (1998)
[7] H. Sillescu, J. Non-Cryst. Solids 243, 81 (1999)
[8] M. Ediger, Annu. Rev. Phys. Chem. 51, 99 (2000)
[9] A. Heuer and K. Okun, J. Chem. Phys. 106, 6176 (1997)
[10] D. N. Perera and P. Harrowell, J. Non-Cryst. Solids 235, 314 (1998)
[11] C. Donati, J. F. Douglas, W. Kob, S. J. Plimpton, P. H. Poole and S. C. Glotzer, Phys. Rev. Lett. 80, 2338 (1998)
[12] C. Bennemann, C. Donati, J. Baschnagel and S. C. Glotzer, Nature 399, 246 (1999)
[13] C. Donati, S. C. Glotzer, P. H. Poole, W. Kob, S. J. Plimpton, Phys. Rev. E 60, 3107 (1999)
[14] Y. Gebremichael, T. B. Schrøder, F. W. Starr and S. C. Glotzer, Phys. Rev. E 64, 051503 (2001)
[15] Y. Gebremichael, M. Vogel and S. C. Glotzer, J. Chem. Phys. (in press)
[16] N. Giovambattista, S. V. Buldyrev, F. W. Starr and H. E. Stanley, Phys. Rev. Lett. 90, 085506 (2003)
[17] M. Aichele, Y. Gebremichael, F. W. Starr, J. Baschnagel and S. C. Glotzer, J. Chem. Phys. 119, 5290 (2003)
[18] B. W. H. van Beest, G. J. Kramer, R. A. van Santen, Phys. Rev. Lett. 64, 1955 (1990)
[19] J.-L. Barrat, J. Badro and P. Gillet, Molecular Simulation 20, 17 (1997)
[20] K. Vollmayr, W. Kob and K. Binder, Phys. Rev. B 54, 15808 (1996)
[21] J. Horbach, W. Kob and K. Binder, J. Non-Cryst. Solids 235-237, 320 (1998)
[22] J. Horbach and W. Kob, Phys. Rev. B 60, 3169 (1999)
[23] J. Horbach and W. Kob, Phys. Rev. E 64, 041503 (2001)
[24] I. Saika-Voivod, P. H. Poole and F. Sciortino, Nature 412, 514 (2001)
[25] G. H. Fredrickson and H. C. Andersen, Phys. Rev. Lett. 53, 1244 (1984)
[26] M. Vogel and S. C. Glotzer (in preparation)
[27] K.-U. Hess, D. B. Dingwell and E. Rössler, Chem. Geol. 128, 155 (1996)
[28] J. C. Mikkelsen, Appl. Phys. Lett. 45, 1187 (1984)
[29] G. Brebec, R. Seguin, C. Sella, J. Bevenot, J. C. Martin, Acta Metall. 28, 327 (1980)
[30] K. Schmidt-Rohr and H. W. Spiess, Phys. Rev. Lett. 66,

3020 (1991)
[31] F. H. Stillinger and J. A. Hodgdon, Phys. Rev. E 50, 2064 (1994)